Synthesis and characterization of FeMn-pinned spin valve arrays

Huixin Wang[a)]
Key Laboratory of Materials Physics, Institute of Solid State Physics, Chinese Academy of Sciences, P.O. Box 1129, Hefei 230031, People's Republic of China

Yucheng Wu
School of Materials Science and Engineering, Hefei University of Technology, Hefei 230009, China

Qingshan Li
Department of Physics, Qufu Normal University, Qufu 273165, China

Ming Wang, Guanghai Li, and Lide Zhang
Key Laboratory of Materials Physics, Institute of Solid State Physics, Chinese Academy of Sciences, P.O. Box 1129, Hefei 230031, People's Republic of China

(Received 15 December 2005; accepted 28 June 2006; published online 1 August 2006)

We have prepared by electrodeposition nanoscale spin valves into the pores of anodic alumina membranes. Aligned nanometric spin valve arrays, well characterized by field emission scanning electron microscopy, are vertical with respect to the plane of the template and exhibit a perfect two-dimensional array with a hexagonal pattern. The largest value of room temperature giant magnetoresistance (GMR) we achieved is 6.8% at 75 Oe. The relatively low saturation fields together with relatively large GMR should make such structures attractive for sensor applications. © *2006 American Institute of Physics*. [DOI: 10.1063/1.2236275]

There has been a considerable amount of interest in spin valve (SV) films, since spin valve films have been demonstrated to be candidates for read heads in magnetic recording systems because of their extra high sensitivity and fairly simple structure for mass production.[1–3] In recent years, the requirement for high density recording heads has driven the research to the nanoscale.[4] Several research works have reported on submicron SVs fabricated by lithography techniques and presented a preliminary study of their transport property.[5] However, decreases in GMR for SV (Ref. 6) and multiplayer[7] nanowires prepared by lithographic techniques have been reported. This was thought to be due to the heating effects at the wire edges during ion milling. To overcome this problem, we describe an alternative method for producing nanoscale SV arrays by template synthesis (using a wet process such as anodization and electrodeposition) instead of the conventional dry process such as e-beam and laser lithography. Furthermore, the electrodeposition techniques with template have great advantages for industrial applications requiring high productivity and mass production of nanostructures at low cost. In this letter, we report on the preparation and magnetotransport properties of $Ni_{80}Fe_{20}/Co/Cu/Co/Ni_{80}Fe_{20}/Mn_{50}Fe_{50}$ nanometric SV arrays by electrodeposition in the self-assembled alumina templates.

The porous anodic aluminum oxide (AAO) templates were prepared by using a modified two-step anodization process.[8] High-purity Al foils (99.999%, 0.3 mm thick) were anodized in 0.3*M* oxalic acid solution at 14 °C at a constant applied voltage of 40 V for 10 h. After removing the resultant aluminum oxide film formed by the first anodization, one side of the Al plate was coated with manicure. A second anodization was performed for 5 h under the same conditions as the first one. The bottom oxide of the AAO templates exposed after removing the aluminum was also removed by dipping in a phosphoric acid solution. A thin Ta layer (thickness 50 nm), which serves as an electrical contact and seed layer for the grown nanoscale spin valves, was sputtered on the surface of the template.

In order to avoid codeposition of Cu in the NiFe and MnFe layers, in this letter, the electrodeposition was carried out in separate baths. The first bath contained $FeSO_4 \cdot 7H_2O$, $MnSO_4$, and $(NH_4)_2SO_4$ solution for plating the MnFe layer. The second bath contained $FeSO_4 \cdot 7H_2O$, H_3BO_3, $NiSO_4 \cdot 6H_2O$, and $NiCl_2 \cdot 6H_2O$ for plating the NiFe layer. The third bath contained H_3BO_3 and $CoSO_4 \cdot 7H_2O$ for plating the Co layer. The fourth bath contained H_3BO_3 and $CuSO_4 \cdot 5H_2O$ for plating Cu layer (spacer layer). To prevent oxidation of the ferrous material to ferric material, when depositing NiFe and FeMn, an inhibitor, such as citric acid or ascorbic acid, was added to the solution. The composition ratios of $Ni_{80}Fe_{20}$ and $Mn_{50}Fe_{50}$ were determined by energy dispersive x-ray (EDX) microanalysis. The electrodeposition was controlled by a computer. The layer thicknesses were adjusted by controlling the deposition times. To prevent oxidation both samples had a 20-nm-thick Cu coating layer on top. The layer sequence of the specimens is FeMn/NiFe/Co/Cu/Co/NiFe/Cu. The FeMn is the bottom layer. MR ratio is defined as MR ratio$=([(R - R_H(\mathrm{sat}))]/R_H(\mathrm{sat})) \times 100\%$. To measure the magnetoresistance of the sample two electrical contacts are placed on the side of the membrane opposite to the Ta coating and a small current passed through the nanowires beneath the contacts. To achieve a measurable change in magnetoresistance it is important for the contacts to have a small overall area. The applied magnetic field dependence of resistance at different temperatures was measured on a Quantum Design superconducting quantum interference device (SQUID) MPMS system. The structure and morphology of nanometric spin valve arrays are characterized by x-ray diffractometer (XRD) and field emission scanning electron microscopy (FESEM).

A field emission scanning electron micrograph of a porous alumina template is shown in Fig. 1(a), from which it is

[a)]Electronic mail: wanghx@issp.ac.cn

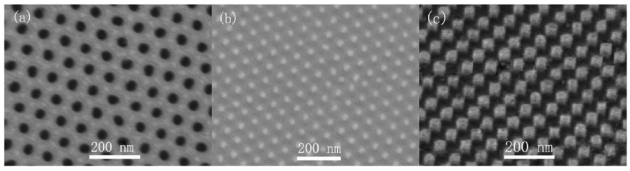

FIG. 1. SEM images: (a) the plan view of the anodic alumina membrane, (b) the plan view of nanometric spin valve arrays, and (c) the side view of nanometric spin valve arrays

found that the nanopores are uniform and highly ordered with pore diameter and interpore distance about 60 and 110 nm, respectively. To obtain the SEM image of the nanometric spin valve arrays, after electrodeposition the sample was dipped into a solution of 5 wt % NaOH to dissolve the upper part or anodic alumina membrane completely. As shown in Fig. 1(b) (plan view) and Fig. 1(c) (side view), the nanometric spin valve arrays are very uniform in diameter, parallel, tidily aligned, uniformly distributed, and exhibit a perfect two-dimensional array with a hexagonal pattern.

A disadvantage of the NiFe/Cu/NiFe/MnFe spin valve is that substantial degradation occurs upon annealing due to intermixing of Ni and Cu.[9] Co and Cu, on the other hand, are immiscible, and significant improvements in thermal stability have been realized by interposing thin Co layers at the interfaces of NiFe/Cu/NiFe GMR bilayers.[10] The present work was based on a rather common type of spin valve structure, $FeMn/Ni_{80}Fe_{20}/Co/Cu/Co/Ni_{80}Fe_{20}$. The bottom two magnetic films (Co and $Ni_{80}Fe_{20}$) are pinned by exchange bias from the FeMn, and the top two magnetic films are free to switch at low applied fields (unpinned). Adjacent Co and $Ni_{80}Fe_{20}$ films are coupled so strongly that they always switch as a single magnetic unit.

Figure 2 shows the XRD patterns as a function of annealing temperature. Samples were annealed at 200, 300, and 400 °C for 30 min in a high-vacuum oven. An external magnetic field of 400 Oe was applied to induce the exchange coupling. All samples showed two strong peaks. Compared

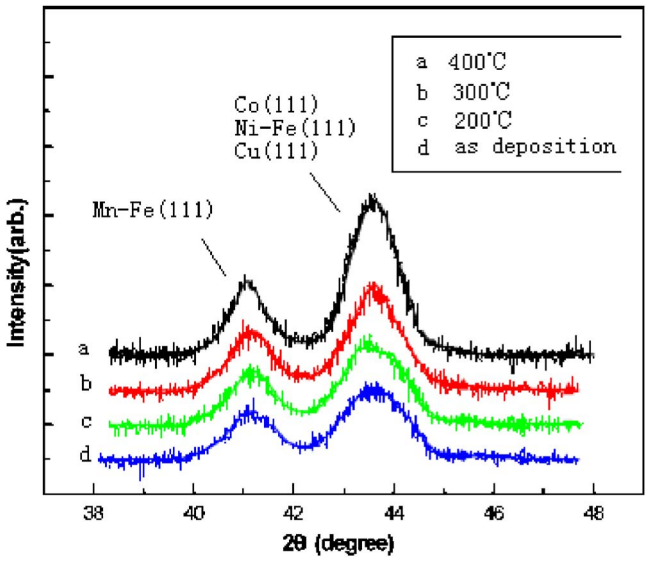

FIG. 2. (Color online) XRD patterns of the nanometric spin valve arrays as a function of annealing temperature.

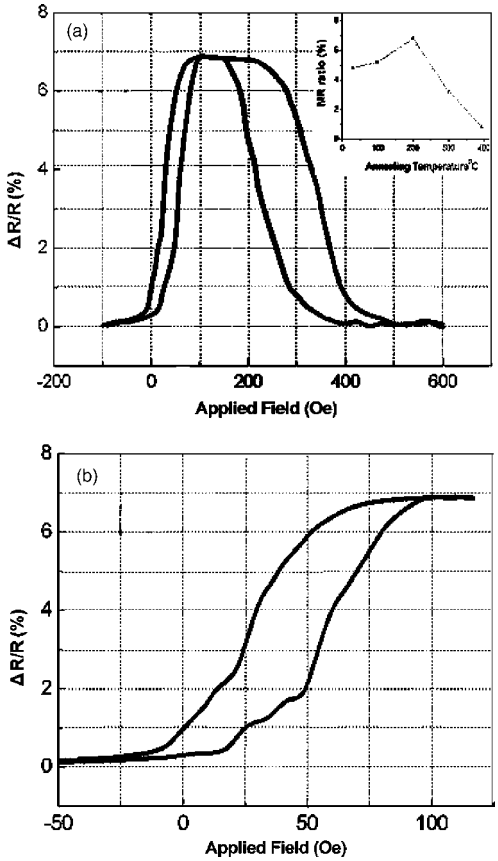

FIG. 3. GMR response of the nanometric spin valve arrays for (a) the high-field case in which both pinned and unpinned magnetic films undergo switching and (b) the low-field case in which only the unpinned magnetic films undergo switching. The inset shows the variation of GMR with annealing temperature.

with the peak positions of standard Ni–Fe, Mn–Fe, Cu, and Co, one of the observed peaks is found to be close to the peak positions of the γMn–Fe (111) with fcc structure and the other is the (111) diffraction peaks of the Co, Ni–Fe, and Cu layers with fcc structure. The second peak for the lowest annealing temperature (200 °C) is actually made up of two peaks, indicating that one can distinguish between the Cu and FeNi. The fact that the other samples do not have this splitting indicates increased interdiffusion with increasing annealing temperature. The peak heights for the NiFe (ll1), Cu (lll), Co (lll), and the γFeMn (lll) increase with annealing temperature. These effects may be due to increased crystallinity or to increased roughness that would make the effective thickness of some parts of the films thicker. It is likely that the crystallites of γFeMn are not well formed in the as-deposited condition at room temperature. Through heat treatment, the epitaxial nature may increase and it leads to the fcc crystalline structure, which may aid to produce high exchange (Hex) bias field.[11]

Figures 3 shows room temperature GMR curves of the nanometric spin valve arrays annealed at 200 °C with structure Cu 20 nm/$Ni_{80}Fe_{20}$ 10 nm/Co 2 nm/Cu 2 nm/Co 2 nm/$Ni_{80}Fe_{20}$ 5 nm/$Mn_{50}Fe_{50}$ 10 nm. In the high-field case [Figs. 3(a)] the magnetoresistance response consist of two loops. The first one corresponds to the rather soft free layer (top two magnetic films) of the SV, which switches from parallel to antiparallel to produce the increase in resistance. The second loop, with an exchange shift of 300 Oe due to exchange coupling between bottom ferromagnetic layers (Co

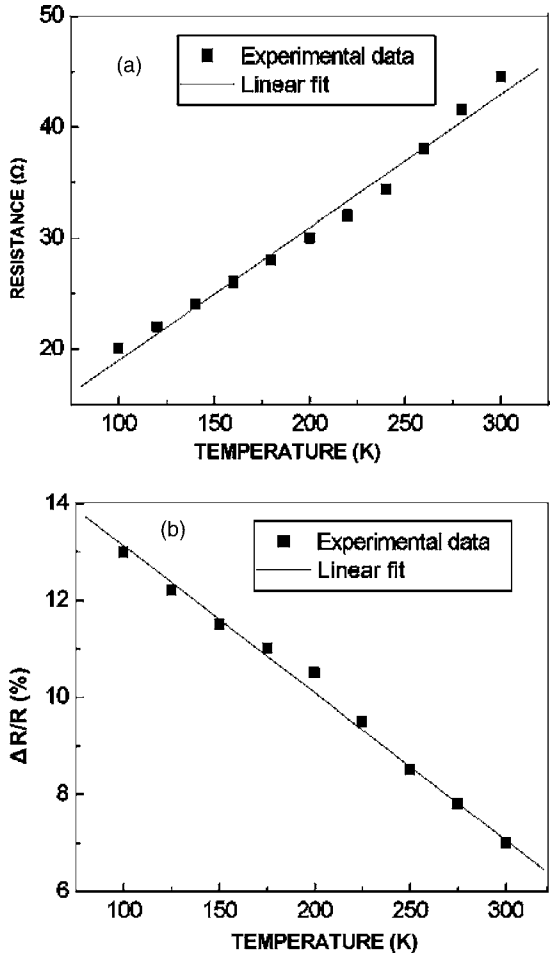

FIG. 4. Temperature dependence of the maximum resistance (a) and the GMR ratio (b) for the nanometric spin valve arrays.

and $Ni_{80}Fe_{20}$) and the antiferromagnetic FeMn layer, corresponds to the reversal of the magnetizations of the pinned layer. The largest value of GMR we achieved is 6.8% at room temperature at 75 Oe, which is much greater than that of submicron spin valve structures prepared by lithography techniques.[12] The inset in Fig. 3(a) shows the change of GMR as a function of annealing temperature. MR ratio started to increase with annealing temperature from 4.7% to 6.8% until 200 °C and exhibited value a of 0.8% at 400 °C. Until 200 °C, improved MR ratio results from the disappearance of the intermixed region. The Cu atoms in the Co matrix diffuse out to the Cu matrix during heat treatment and the Co layer recovers its magnetization.[11] At 400 °C, decreased MR ratio is due to increased interdiffusion and intermixing layer. This is in agreement with the x-ray measurements in Fig. 2.

Figure 3(b) presents the low-field GMR loops for the same sample as in Fig. 3(a) at room temperature. The center of the loop is shifted from zero field due to the ferromagnetic coupling through the Cu interlayer. The slight tilt of the magnetoresistance loop is mainly attributed to the inhomogeneities among the wires, which decrease the sensitivity of GMR response slightly. The relatively low saturation fields together with the relatively large GMR should make such structures attractive for sensor applications.

Figure 4 shows the dependence of the maximum resistance (a) and MR (b) on temperature for the sample annealed at 200 °C. As is typical for metals, the quasilinear resistance increases with temperature because of phonon and magnon scatterings. A striking result is the nearly linear variation of the GMR with temperature. Such a quasilinear decrease was observed by Dieny[13] This increase of magnetoresistance with decreasing temperature mostly reflects the decreasing scattering and depolarization by spin waves and phonons and thus the increasing relative contribution of spin-dependent scattering.[14]

In conclusion, by serving the nanochannel of the anodic alumina membranes as a microcell, highly ordered nanometric spin valve arrays have been fabricated. The results of field emission scanning electron microscopy indicated that the nanometric spin valve arrays were highly ordered. GMR ratios as high as 6.8% have been obtained at room temperature at 75 Oe. These relatively low-field values together with the relatively large GMR should make such structures attractive for sensor applications.

This research was supported by National Major Project of Fundamental Research: Nanomaterials and Nanostructures (Grant No. 19994506).

[1] E. B. Myers, D. C. Ralph, J. A. Katine, R. N. Louie, and R. A. Buhrman, Science **285**, 867 (1999).
[2] S. O. Valenzuela, D. J. Monsma, C. M. Marcus, V. Narayanamurti, and M. Tinkham, Phys. Rev. Lett. **94**, 196601 (2005).
[3] J. A. Katine, F. J. Albert, R. A. Buhrman, E. B. Myers, and D. C. Ralph, Phys. Rev. Lett. **84**, 3149 (2000).
[4] W. C. Uhlig and J. Shi, Appl. Phys. Lett. **84**, 759 (2004).
[5] N. Smith, V. Synogatch, D. Mauri, J. A. Katine, and M. C. Cyrille, J. Appl. Phys. **91**, 7454 (2002).
[6] L. Kong, Q. Pan, B. Cui, M. Li, and S. Y. Chou, J. Appl. Phys. **85**, 5492 (1999).
[7] J. A. Katine, A. Palanisami, and R. A. Buhrman, Appl. Phys. Lett. **74**, 1883 (1999).
[8] H. Masuda, and M. Satoh, Jpn. J. Appl. Phys., Part 2 **35**, L126 (1996).
[9] V. S. Speriosu, J. P. Nozieres, B. A. Gurney, B. Dieny, T. C. Huang, and H. Lefakis, Phys. Rev. B **47**, 11579 (1993).
[10] B. Dieny, J. Magn. Magn. Mater. **136**, 335 (1994).
[11] Hong Jin Kim, Jun Soo Bae, Taek Dong Lee, and Hyuck Mo Lee, J. Magn. Magn. Mater. **241**, 173 (2002).
[12] D. Morecroft, B. B. Van Aken, J. L. Prieto, D.-J. Kang, G. Burnell, and M. G. Blamirea, J. Appl. Phys. **97**, 054302 (2005).
[13] B. Dieny, J. Magn. Magn. Mater. **151**, 378 (1995).
[14] B. Dieny, V. S. Speriosu, S. Metin, S. S. P. Parkin, B. A. Gurney, and P. Baumgart, J. Appl. Phys. **69**, 4774 (1991).